

# Swissmetro : aerodynamic drag and wave effects in tunnels under partial vacuum

Michele Mossi (\*), Stefano Sibilla (\*\*)

(\*)GESTE Engineering SA, Scientific park PSE-C  
CH - 1015 Lausanne, Switzerland  
Phone +41 021 693 83 60 Fax +41 021 693 83 61 e-mail: [michele.mossi@geste.ch](mailto:michele.mossi@geste.ch)

(\*\*) Dipartimento di Ingegneria Idraulica e Ambientale, Università di Pavia  
via Ferrata, 1 27100 Pavia, Italy  
Phone +39 0382 50 57 62 Fax +39 0382 50 55 89 e-mail: [stefano.sibilla@unipv.it](mailto:stefano.sibilla@unipv.it)

## Keywords

**Aerodynamics, drag, partial vacuum, pressure wave, Swissmetro.**

## Abstract

The maximum allowed train velocity for given vehicle and tunnel cross-section areas is limited by aerodynamic effects. These effects influence the train power requirement, the traction energy costs, the pressure wave amplitude and, in a second time, the temperature evolution into the tunnel. The knowledge of the unsteady aerodynamic field around the train is therefore essential to the optimum choice of a tunnel configuration, and mainly of the cross-section diameter and of the presence and position of pressure relief ducts. In this paper, the aerodynamic field generated by a high-speed train travelling under partial vacuum through the Basle-Zurich Swissmetro tunnel are analysed by means of quasi one-dimensional numerical simulations of the induced air flow and thus of the computational domain. Several tunnel configurations at high blockage ratio are discussed, together with the positive and negative effects of pressure relief ducts and of partial air vacuum. Results suggest that configurations consisting of twin tunnels connected by pressure relief ducts near the end stations should be preferred.

## 1 Introduction

The development of new transportation technologies and the improvement of the existing systems in the railway field have led to the increase of the commercial speed, and therefore to the design and building of new high-speed railway and Maglev (Magnetic levitation train) lines. These new lines need straighter tracks and thus require longer and more numerous tunnel sections in order to avoid obstacles and to reduce environmental impacts [1]. Examples include the tunnels to be built through the Alps (the Lyon-Torino connection with a 54 km long tunnel [2] or the Swiss AlpTransit project with about 120 km of tunnels) and the new Maglev Yamanashi test line in Japan, which has 82% of tunnels on 42.8km [3].

Some aerodynamic problems are peculiar to the passage of a high-speed train in a tunnel and do not appear in open air: compression and expansion waves are generated when the train enters the tunnel, when its velocity changes and wherever the tunnel cross-section is varied. These pressure waves cause relevant aerodynamic loads on vehicle and tunnel structures. Aerodynamic noise, forces and moments acting on the train, and especially the aerodynamic drag, grow due to the

confinement of the surrounding space. These aerodynamic phenomena gain in complexity and importance as the train speed and the blockage ratio (ratio of vehicle to free tunnel cross-section area) increase.

Aerodynamic drag is by far the major contribution to the total drag for high-speed trains travelling in tunnels; the entity of this drag [4, 5] depends on several parameters such as the blockage ratio, the tunnel network geometry and surface, the number of pressure relief ducts, the train type and its speed, the presence of other trains, etc. If this drag is underestimated during design, either the required operating speed can not be attained, or the air temperature resulting from the dissipated power can exceed safety limits. Such negative effects can be minimized by reducing the blockage ratio (i.e. by increasing the tunnel diameter), or by connecting the tunnel to the atmosphere, or to a second parallel tunnel. However, the need to keep building costs low requires the reduction of the tunnel diameter. If the train velocity is not diminished, this reduction enhances unsteady aerodynamic problems: the amplitude of pressure waves grows and pressurized vehicles could be required; the air flow velocity increases and unsteady compressible effects become dominant; moreover, the train drag rises, leading to extremely high power requirements for high-speed motion, eventually limiting the maximum speed allowed by the power supply system.

However, in densely populated areas and in mountainous regions such as Switzerland, tunnels are the only practicable possibility for high-speed railway connections.

A solution that allows the tunnel diameter to remain small while reducing the effect of pressure waves and avoiding a rise in aerodynamic drag, can then be envisaged in running high-speed trains in low-pressure closed tunnels, as proposed by the Swissmetro project [6]. Swissmetro consists in a high-speed underground transport network which would be composed by high blockage ratio tunnels (about 0.4) under a partial vacuum of about 1/10 of the atmospheric pressure. In these tunnels, pressurised Maglev vehicles will move at speed higher than 100 m/s and will be able to carry 400 seated passengers in perfect safety.

The management of the Swissmetro project is now analysing the technical and economical feasibility of a high-speed connection between the city-centres of Basle and Zurich. This line, which could be in operation in 2020, will be composed by two parallel, 89.1 km long tunnels of 5 m interior diameter, one tunnel of each direction.

The present study is focused on this line and is aimed at the analysis of aerodynamic phenomena occurring during the cruise of the Swissmetro vehicle. Our analysis follows the suggestions of a previous study on the effect of different tunnel configurations on the aerodynamic drag of very high-speed trains [7]. The approach used in the present work consists in a numerical analysis using a quasi one-dimensional finite volume model of air flow and train motion in the tunnel [8]: the emphasis of the work is therefore on the tunnel design, rather than on the detailed aerodynamic phenomena on the train itself.

## **2 Physical model and numerical solution**

The flow generated by a train which travels inside a railway tunnel is unsteady, compressible, three-dimensional and turbulent. Pressure, density and velocity fields around the train are affected by the confining effects of the tunnel walls even at steady state; moreover, unsteady phenomena develop whenever the relative motion between train and tunnel imposes strongly unsteady boundary conditions to the flow. This is the case when the train ends cross the tunnel portals, when train passing occurs in the same tunnel and, in general, whenever the tunnel section changes or when the tunnel is connected with a different tunnel or atmosphere. In these circumstances, pressure waves are generated: these waves propagate at the local speed of sound, interfere with each other and reflect within the tunnel in a complex way [9, 10].

A correct description of the flow requires the solution of the three-dimensional unsteady equations of gas dynamics. However, experimental evidence shows that, if the tunnel length is much larger than its hydraulic diameter, the propagation of pressure disturbances takes place by means of approximately plane waves and the instantaneous distribution of the fluid dynamic variables is nearly uniform in each tunnel section, while intrinsically three-dimensional features are concentrated only in the close vicinity of the train and tunnel ends and in those regions where the tunnel walls have a complex shape, i.e. abrupt changes of the cross-section area, mutual connections between tunnels, tunnel connections with the atmosphere [11, 12].

As a consequence, the large-scale behaviour of the flow in a train-tunnel system can be reasonably predicted by using quasi one-dimensional models, obtained by coupling a one-dimensional mean flow description with suitable corrective models, capable of capturing the local three-dimensional features of the flow in some peculiar regions of the flow field. The governing equations are a modified version of the Euler equations in which source terms for distributed and localized friction effects are introduced. The resulting system is discretised in space by a second-order accurate finite-volume scheme, and is solved in time through a 5-stage Runge-Kutta scheme, which is also second-order accurate [7, 8].

### 3 Test case characteristics

This paper discusses numerical results obtained on different possible tunnel configurations on the Basle-Zurich line (see Figure 1 and Table 1). The distance between the end stations is 89.1 km; the stations are considered to be 150 m long, with a circular cross section of 7 m diameter. These different tunnel configurations include single-track tunnels either with or without connections with other parallel tunnels. Each main tunnel has a circular cross section of 5 m diameter. Its walls have been considered adiabatic, with a friction coefficient of 0.003, corresponding to a mean wall roughness of 0.5 mm. Pressure relief ducts, when present, are 25 m long, cylindrical of 4 m diameter, and connect perpendicularly two main tunnels with equal section. Their friction coefficient is 0.005, higher than that of the main tunnel, to take into account the fact that these short ducts are usually bored manually.

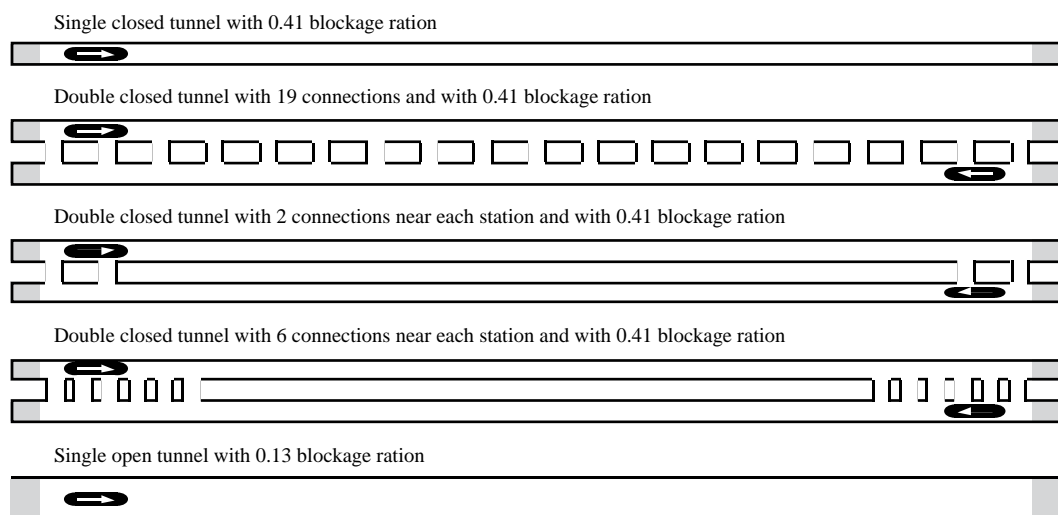


*Figure 1 – The different tunnel configurations analysed (not to scale). Gray indicates the position of the end stations.*

Tunnel Configuration	Tunnel length [km]	End conditions	Interior tunnel diameter [m]	Blockage ratio	Pressure level [Pa]
Single closed tunnel (SCT)	89.1	Closed	5.0	0.41	10'000
Double closed tunnel (DCT-19)	89.1	Closed	5.0	0.41	10'000
Double closed tunnel (DCT-2x2)	89.1	Closed	5.0	0.41	10'000
Double closed tunnel (DCT-2x6)	89.1	Closed	5.0	0.41	10'000
Single open tunnel (SOT)	89.1	Open	8.9	0.13	101'300

*Table 1 – The different tunnel configurations analysed.*

Each train running in the system is symmetric and 130 m long: its nose and tail are 15 m long and its core has a circular cross section of 3.2 m diameter; the resulting blockage ratio in the tunnel is 0.41. The train leaves from Basel, accelerates steadily at  $1.11 \text{ m/s}^2$  for 100 s, reaching its cruise speed of 111.1 m/s (400 km/h); the deceleration is performed at the same rate; the arrival at Zurich station occurs after 800 s.

## 4 Results and discussion

### 4.1 Single closed tunnel

The simplest tunnel configuration under partial vacuum consists in a single tunnel closed at both ends and directly connecting the end stations (SCT, see Figure 1 and Table 1). The high blockage ratio leads to a pronounced piston effect [1, 7]: the air pushed ahead of the train causes a significant pressure increase in front of the train nose and creates a pressure decrease in the wake behind the tail (Figure 2), while a reduced portion of the air flows around the vehicle. Around the train, the air flow accelerates along the nose and the annular space (Figure 3), reaching a peak velocity of 215 m/s (in the vehicle-fixed frame of reference) upstream of the train tail; the Mach number reaches there a maximum value of 0.63, indicating the existence of important compressibility effects, although no transonic region appears as in higher blockage ratio flows [7].

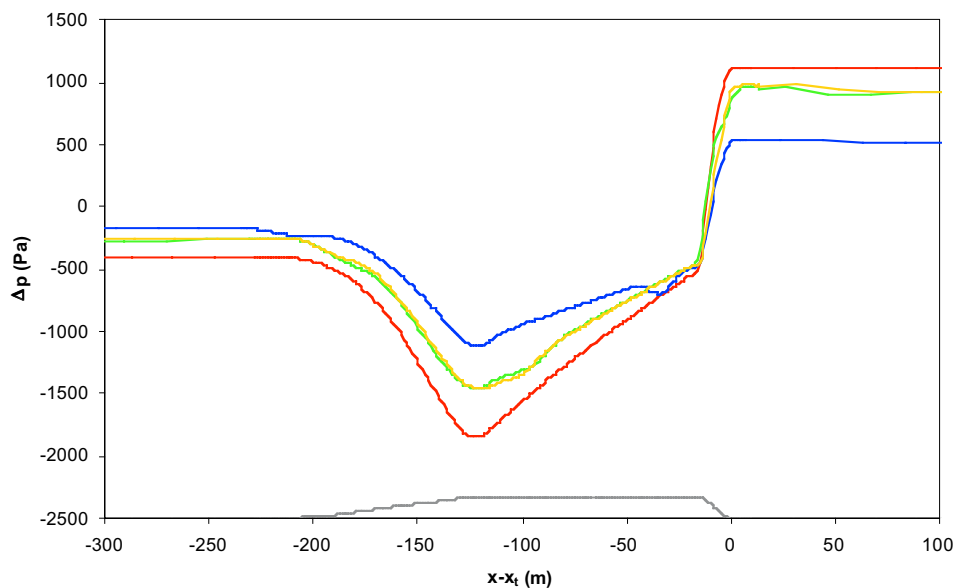


*Figure 2 – Pressure distribution past the train in the vehicle-fixed frame of reference at time  $t=450 \text{ s}$ . Single tunnel SCT —; double tunnel with 19 connections DCT-19 —; double tunnel with 2 connections near each station DCT-2x2 —; double tunnel with 6 connections near each station DCT-2x6 —; train and train wake position —.*

Pressure-wave evolution can be represented through the pressure variation in front of the train nose (Figure 4). Pressure initially increases in front of the train owing to tunnel friction; in the meanwhile, the pressure wave generated by the initial train acceleration reaches the closed end of the Zurich station and is reflected backwards as a compression wave. When the reflected wave reaches the train nose (at  $t \approx 450$  s), it leads to an increase of the pressure level in front of the train. Due to the piston effect, this increase is accentuated when the train approaches the arrival station, reaching its maximum value of 3210 Pa at the beginning of the deceleration phase.

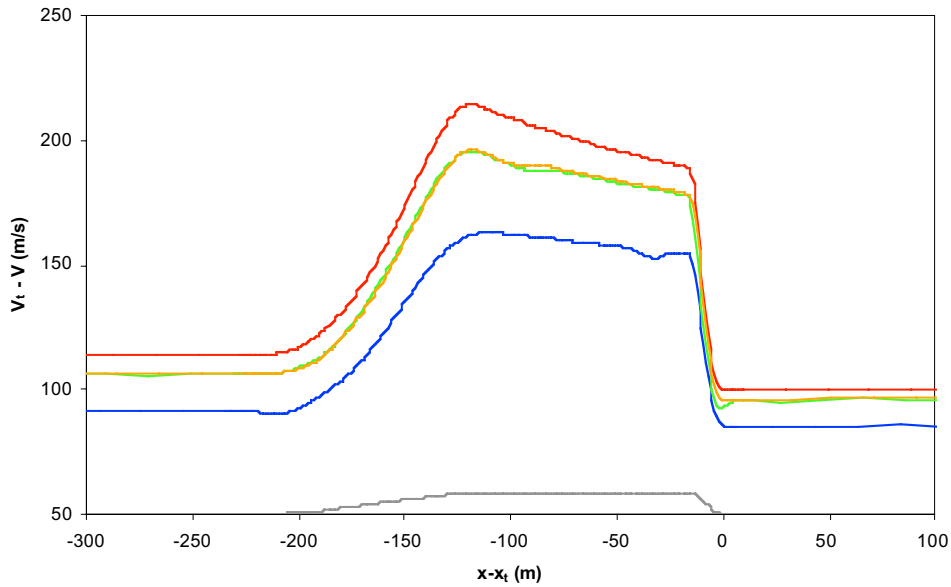


**Figure 3** – Relative velocity distribution past the train in the vehicle-fixed frame of reference at time  $t=450$  s. Single tunnel SCT — ; double tunnel with 19 connections DCT-19 — ; double tunnel with 2 connections near each station DCT-2x2 — ; double tunnel with 6 connections near each station DCT-2x6 — ; train and train wake position — .

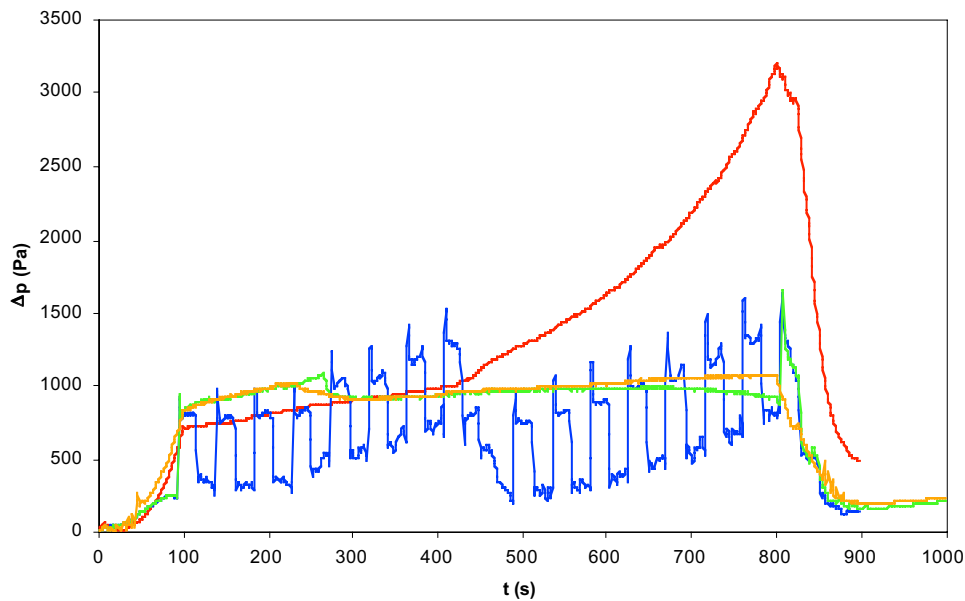


**Figure 4** – Static pressure history 2 m before the high-speed train nose. Single tunnel SCT — ; double tunnel with 19 connections DCT-19 — ; double tunnel with 2 connections near each station DCT-2x2 — ; double tunnel with 6 connections near each station DCT-2x6 — .

As shown in Figure 5, aerodynamic drag and power evolution resemble the pressure one: drag increases sharply for  $t \geq 450$  s until the beginning of the deceleration phase, where it reaches its maximum of slightly more than 40 kN; the same behaviour is shown by the aerodynamic power, which reaches a maximum value of 4.5 MW, while its average value during the cruise phase is 3.3 MW.

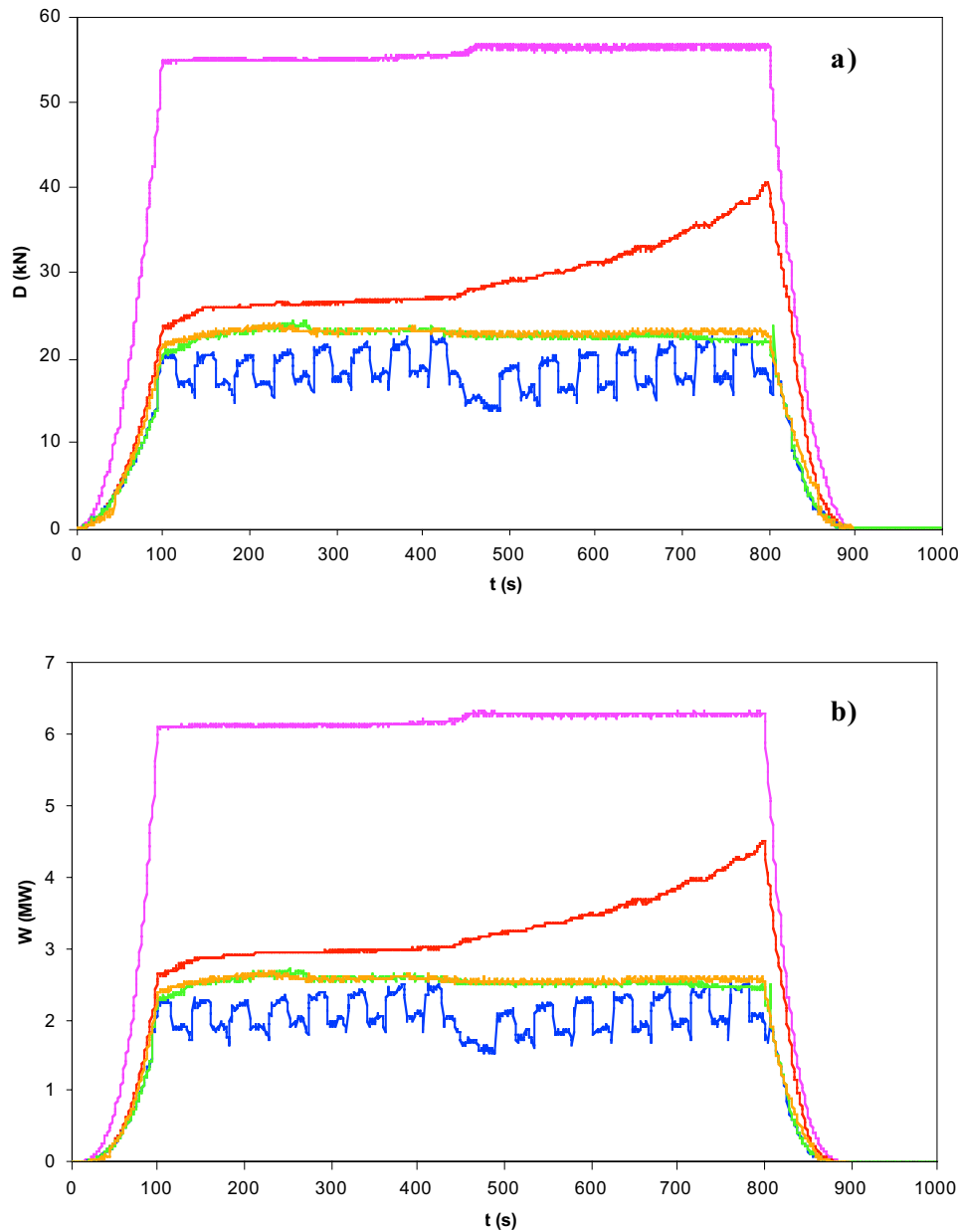


**Figure 5** – Comparison of total aerodynamic drag (a) and power (b) of the different configurations of tunnel networks connecting Basel and Zurich. Single tunnel SCT —; double tunnel with 19 connections DCT-19 —; double tunnel with 2 connections near each station DCT-2x2 —; double tunnel with 6 connections near each station DCT-2x6 —; open tunnel with 0.13 blockage ratio at atmospheric pressure (1 atm) —.

The effect of the introduction of partial vacuum in the tunnel system can be evaluated by comparing the closed tunnel results with the power which would be required to obtain the same cruise speed in an open tunnel, at atmospheric pressure and at a lower blockage ratio. A conventional blockage ratio of 0.13 has been chosen for this comparison, resulting in an open-tunnel cross-section diameter of 8.9 m. In this case, the weaker pressure wave generated at the train departure from Basle is reflected as an expansion wave at the Zurich tunnel portal; a steady

outgoing air flow is also induced at the same portal, and the piston effect is therefore reduced. Nevertheless, Figure 5 shows that aerodynamic drag and power appear to be still higher than the high-blockage partial vacuum case: the required power soon reaches a value of 6.1 MW which is maintained for most of the train cruise in the tunnel (see also Table 2).

In conclusion, compared with the open configuration at atmospheric pressure, the introduction of a 10'000 Pa partial air vacuum in the tunnel leads to a reduction of the peak level of the required power which is 74% of the corresponding value in an open tunnel with a conventional blockage ratio. Therefore this configuration already yields an important reduction of both construction costs and energy requirements.

## 4.2 Tunnel network with connections

As successfully applied for the Channel tunnel [13], good results in terms of piston-effect reduction can be obtained by coupling the main tunnel with another single-track parallel tunnel through an array of pressure relief ducts (see Figure 1). In the twin tunnels, trains move in opposite directions; therefore, the interaction between trains strongly influences the air flow: here, for simplicity, the train motion is considered perfectly synchronized.

In the present study, the number of secondary ducts is kept as low as possible, compared with the benefits in aerodynamic drag reduction, to limit unwanted raising of construction costs and to guarantee an easy isolation of both tunnels for safety or maintenance (we remember that both tunnels are under partial air vacuum in operational conditions; however, for safety or maintenance, the pressure level in a single tunnel could be increased up 1 atm). A configuration having one connection every 5 km between the parallel tunnels (DCT-19) is considered representative of this compromise. The first connections are situated just after the end of each station to reduce the high pressure levels which occur in the arrival stations when the trains are approaching. The total number of connections is thus 19.

The presence of pressure relief ducts allows the generation of an air flow in the second tunnel from the high pressure regions in front of the train nose to the low pressure regions behind the tail. This alleviates the piston effect, thus reducing the pressure drag and the required power, as can be observed in Figure 5. The improvement with respect to the single tunnel case (SCT) is therefore very important: the peak power is reduced to 2.5 MW (i.e. by a factor 1.8), the average one to 2.1 MW. The peak value occurs at the last connection before the train crossing, instead of occurring at the beginning of the train deceleration phase.

A major drawback of this configuration is the strong drag increment on the train at each shaft crossing. These increments occur when the train head crosses a shaft, due to pressure and air velocity differences in the main tunnel on each side of the connection; this drag gradient is very high: in 0.8 s – which is about three quarters of the time needed by the whole train to pass the bifurcation point – the drag can rise by a value close to 4 kN. In a real case, where the train speed is not imposed as constant, these drag fluctuations could result in unwanted sudden deceleration during cruise.

A further crucial problem connected with pressure relief ducts is the cross-flow generated by pressure differences between the tunnels: as shown in Figure 6, this air flow can reach 40 m/s, resulting in a lateral force of several thousand Newtons acting on the train at each shaft crossing. This lateral load, already experienced in very long tunnels like the Channel one, can generate high structural loads and pose problems for train control. These problems can be reduced if the shafts are designed so as to prevent direct impingement of the cross-flow on the train; however, shaft efficiency could also be reduced.

The best way to reduce the impact on the train motion of these inter-tunnel connections, without diminishing their effect, is to locate them where the train speed and the upstream pressure level are not high enough to increase the piston effect and to generate high velocity air flow in the connecting ducts. Two solutions have been tested: the first one consists in placing two ducts along the track 10 m after each station and other two 5 km inside the tunnel (DCT-2x2, see Figure 1); the second one consists in placing an array of 6 ducts every 200 m after each

station (DCT-2x6). Due to the reduced speed of the train at the shaft crossing, the air flow induced through the ducts does not exceed 30 m/s in the first case and 20 m/s in the second. Moreover, the drag rise at the crossing of the inner ducts is eliminated. The required aerodynamic power, very similar for both DCT-2x2 and DCT-2x6 configurations, although 19% higher on average (2.5 MW) than in the DCT-19 configuration, maintains an almost constant value for most of the train cruise (Figure 5).

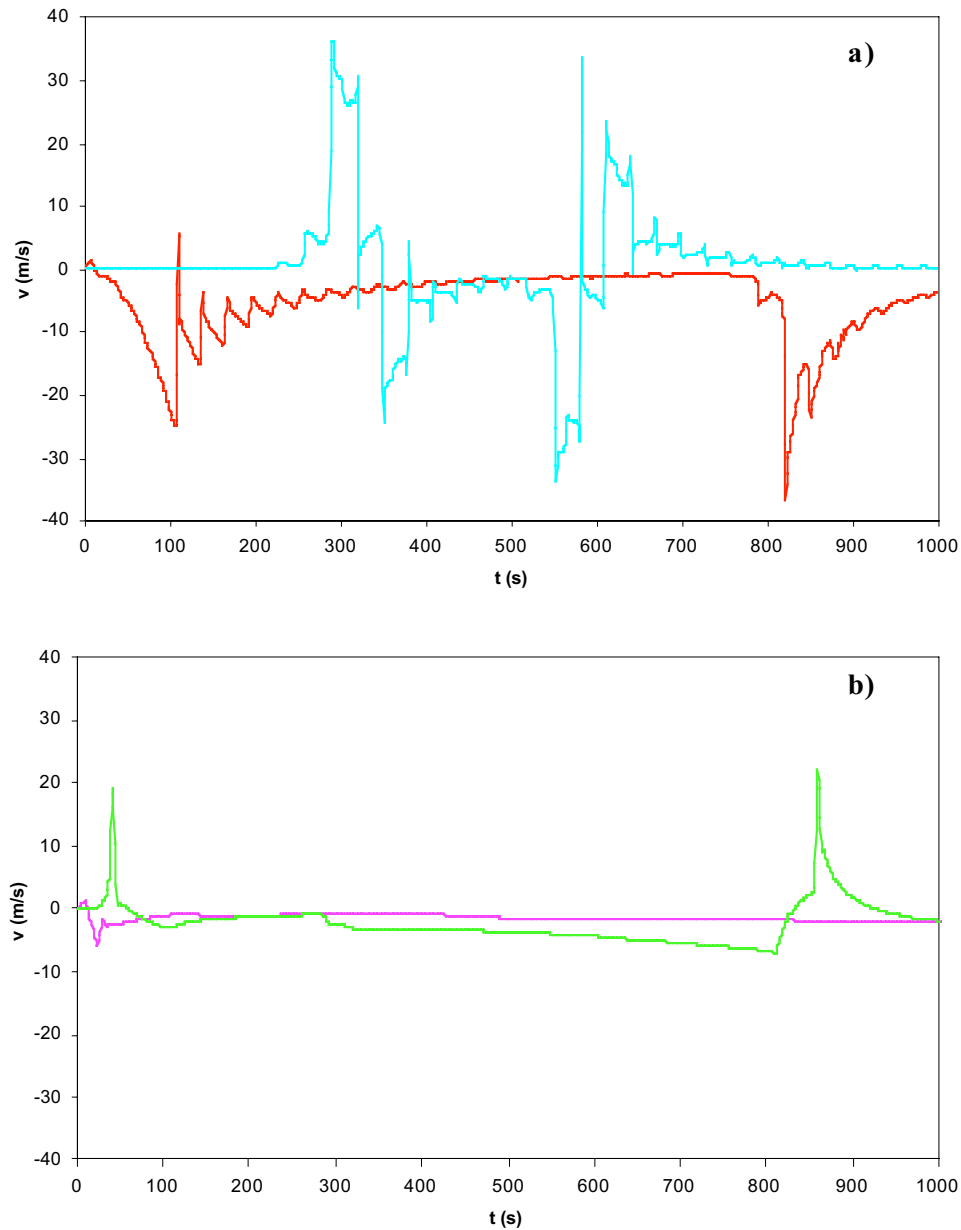


**Figure 6** – Mean air velocity in the middle of pressure relief ducts: (a) double tunnel with 19 connections (DCT-19): 1<sup>st</sup> duct after departure station — red —, duct after 25 km — cyan —; (b) double tunnel with 6 connections near each station (DCT-2x6): 1<sup>st</sup> duct after departure station — magenta —, 6<sup>th</sup> duct after departure station — green —.

To summarise, in order to put out the importance of the tunnel design and the advantages of the reduced pressure level into the Swissmetro tunnel, Table 2 compares the resulting aerodynamic power for different closed and open tunnel configurations.

Tunnel Configuration	Blockage ration	Tunnel diameter [m]	Pressure level [Pa]	Average power [MW]	Maximum power [MW]
Single closed tunnel (SCT)	0.41	5.0	10'000	3.28	4.52
Double closed tunnel (DCT-19)	0.41	5.0	10'000	2.08	2.51
Double closed tunnel (DCT-2x2)	0.41	5.0	10'000	2.53	2.69
Double closed tunnel (DCT-2x6)	0.41	5.0	10'000	2.56	2.67
Single open tunnel (SOT)	0.13	8.9	101'300	6.21	6.31
Single open tunnel	0.07	12.0	101'300	4.51	4.58
Open-air	0.00	$\infty$	101'300	3.48	3.48

*Table 2 – Average and maximum aerodynamic powers for all tunnel configurations.*

The smallest aerodynamic drag is obtained with the DCT-19 configuration; however, as mentioned before, this configuration generates a strong drag increment at each shaft crossing (see Figure 5) and a high-speed cross-flow in the pressure relief ducts due to pressure difference between the tunnels. To reduce the importance of these drawbacks, the configurations DCT-2x2 and DCT-2x6 have been proposed. Both these configurations present a very similar aerodynamic drag, but configuration DCT-2x6 offers the best conditions in term of cross-flow (see above). The average and maximum powers (2.5 and 2.7 MW respectively) are only 40% of those required in the 0.13 blockage ratio configuration at atmospheric pressure (6.2 and 6.3 MW) and are still 25% smaller than in the open-air condition (3.5 MW). Thus, the efficiency of the partial vacuum and of the pressure relief ducts still remains high.

In conclusion, the presence of pressure relief ducts greatly reduces the piston effect, and therefore the aerodynamic drag, in closed configurations under partial vacuum. If the array of pressure relief ducts is only kept close to the end stations, the flow velocity through each connecting duct can be minimized. The aerodynamic drag in these configurations under partial vacuum is much smaller than the one obtained at atmospheric pressure in a standard low-blockage ratio configuration and still in an open-air configuration: the decrease in maximum drag can range from 50% to 60%. However, because of the presence of connections between tunnels, trains travelling in opposite tunnels can reciprocally interact, suffering, in some cases, of high unsteady aerodynamic loads. To minimise this interaction, pressure relief ducts have to be constructed near the end station, where the vehicle speed is relatively low.

### 4.3 Aerothermal loads on stations

The preliminary structural design of tunnel networks under partial vacuum requires a proper evaluation of mechanical and thermal stresses connected with the train motion. Moreover, pressure and temperature stresses in the tunnel network are also needed for the design of the tunnel lining as well as of the station systems connected with train housing, tunnel pressurization and passenger boarding. However, operation under partial vacuum requires a design based on a constant pressure difference of 1 atm at most between passenger areas at atmospheric pressure – i.e. inside trains and stations – and the tunnel. In this case, pressure variations due to train motion do not appear to pose important design constraints, but could generate fatigue problems on the wall structures.

It must be noted that the energy equation is here solved in the hypothesis of adiabatic walls in tunnels and stations, and heat generation by train equipments is neglected: temperature values here reported must therefore be intended as a preliminary and approximate indication of thermal loads on trains and stations.

Pressure evolution in the departure and arrival stations is influenced in an opposite way by the train motion. The departure station (Basle) is immediately reached by the expansion wave generated by the train tail, and by its multiple reflections between the tunnel end and the train itself (Figure 7). This effect is mostly noticeable in the single tunnel case, where a minimal pressure of 9320 Pa is reached; this value corresponds to the highest (negative) pressure load for the vacuum sealing systems in the station. Later, the pressure in the Basle station rises, due to the effect of the reflected initial compression wave and, in the double tunnel configurations, of the piston effect of the second train in the adjacent tunnel. In either case, pressure never reaches

significant values when compared to pressure levels in the arrival station, Zurich, (Figure 8), where the difference between single and double tunnel configurations is more evident.

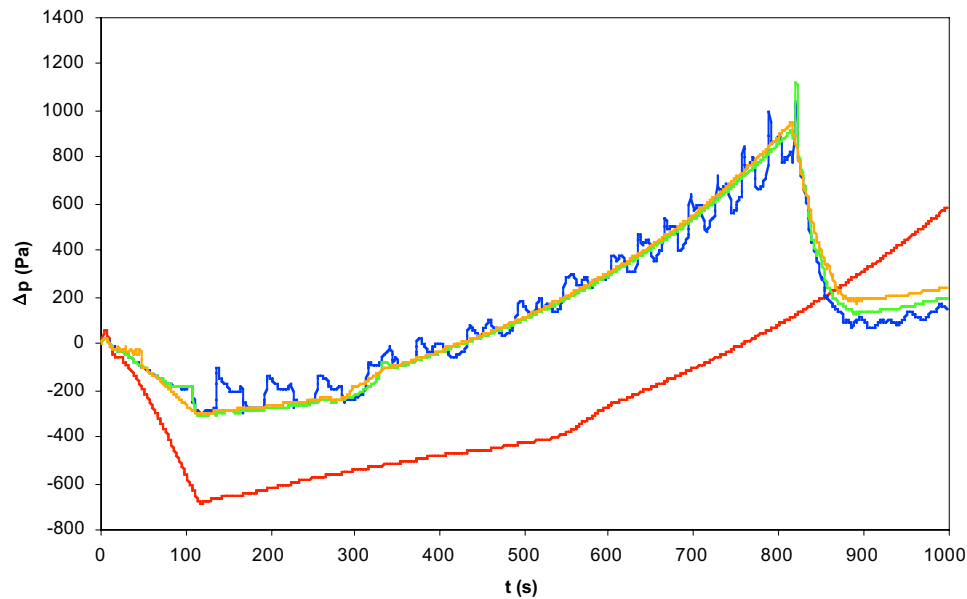


**Figure 7** – Static pressure history in the middle of Basle station (departure station). Comparison between the different configurations of tunnel networks. Single tunnel SCT — ; double tunnel with 19 connections DCT-19 — ; double tunnel with 2 connections near each station DCT-2x2 — ; double tunnel with 6 connections near each station DCT-2x6 — .

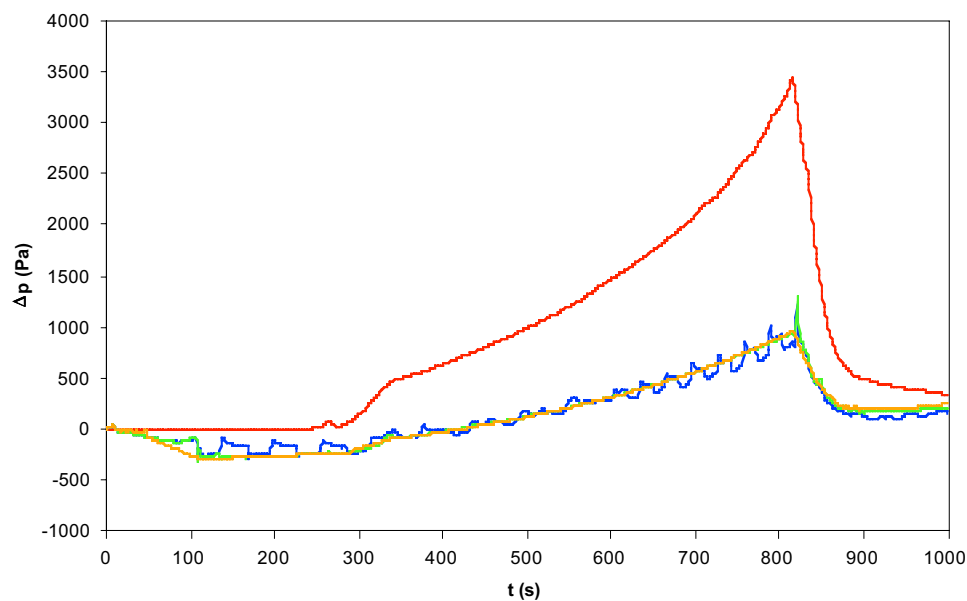


**Figure 8** – Static pressure history in the middle of Zurich station (arrival station). Comparison between the different configurations of tunnel networks. Single tunnel SCT — ; double tunnel with 19 connections DCT-19 — ; double tunnel with 2 connections near each station DCT-2x2 — ; double tunnel with 6 connections near each station DCT-2x6 — .

In single tunnel cases, the flow field in the Zurich station is obviously undisturbed until the arrival of the pressure wave generated by train departure from Basel. In double tunnel configurations, on the other hand, each arrival station is immediately reached by the expansion wave which is generated by the tail of the train leaving the adjacent departure station and transmitted through

the pressure relief ducts; due to the connections between the stations and the train synchronisation, aerodynamic loads in departure and arrival stations are therefore very similar. Peak pressure values in the arrival station reach the same order of magnitude of the corresponding peak values on the train head (Figure 4). Other effects appear when the train departure and movement is not synchronised between the "Basle-Zurich" and the "Zurich-Basle" tunnels. These effects are discussed in [7].

Thermal effects in the arrival station can be quite important: in the single tunnel configuration the estimated peak temperature in the arrival station reaches 25 K more than the undisturbed initial value (Figure 9). In all of the other configurations, however, temperature growths are below 10 K: therefore, they do not appear to pose serious design problems.

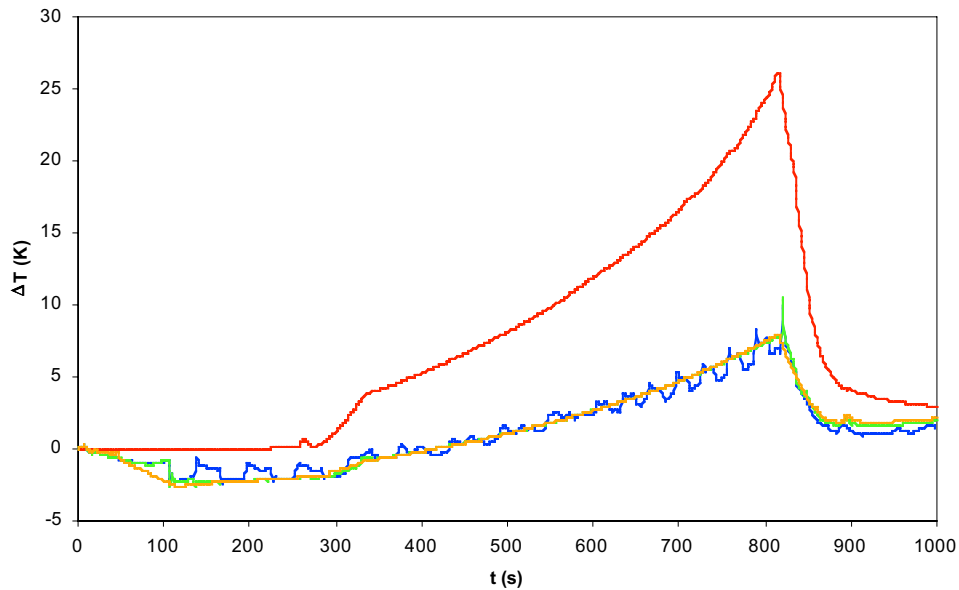


**Figure 9** – Temperature history in the middle of Zurich station. Comparison between the different configurations of tunnel networks. Single tunnel SCT —; double tunnel with 19 connections DCT-19 —; double tunnel with 2 connections near each station DCT-2x2 —; double tunnel with 6 connections near each station DCT-2x6 —.

## 5 Conclusion

The air flow induced by the passage of high-speed trains in the Basle-Zurich Swissmetro tunnel has been predicted by a quasi one-dimensional numerical model in order to establish tunnel design criteria.

The reduction of the diameter of the tunnel is desirable in order to limit construction costs (which can be tentatively considered proportional to the cross-section diameter itself). However, this reduction increases blockage ratios for given train geometries, thus leading to an unwanted rise of propulsion costs. The realization of such tunnel connections under atmospheric conditions appears therefore to be inconvenient due to the high requirements in terms of power supply and to environmental impact at open ends. The construction of underground connections under partial vacuum seems to be the most viable solution to the problem. However, the effects of multiply reflected compression waves on tunnel closed ends can reduce the advantages of partial vacuum in single closed tunnels.

In this framework, the best configuration for this long-range, high blockage ratio tunnel network seems to consist in two coupled tunnels connected by a number of pressure relief ducts. These

connections allow both a reduction of the piston effect generated by the moving train and a positive mutual interaction of trains moving in opposite directions. Furthermore, thanks to a well distribution of the pressure relief ducts, the resulting aerodynamic drag can be even smaller than the one observed in the open-air. The advantages of the partial vacuum are therefore obvious.

Side effects of these connections are not always desirable: sudden increases in aerodynamic drag and strong lateral wind loads on the train can be generated. A solution to this problem can be found by placing pressure relief ducts only in proximity of the stations, where the high-speed train is in its accelerating/decelerating phase. The power required for train motion is, in this case, more than 40% lower than in the single tunnel connection and almost 60% lower than in a single tunnel connection at low blockage ratio and atmospheric conditions.

## References

1. Mossi M., *Simulation of benchmark and industrial unsteady compressible turbulent fluid flows*, Ph.D. Thesis, Ecole Polytechnique Fédérale de Lausanne, 1999
2. Taillé J.Y., Brulard J., Rèty J.M., Fauvel P., *Les recherches techniques pour l'étude de faisabilité du tunnel de base de la liaison transalpine Lyon-Turin*, *Revue Générale des Chemins de Fer*, **197**, 17-27, 1995.
3. Takagi H., *Maglev in Japan - Yamanashi test line*, 2nd National Swissmetro Day, ETH, Zurich, 1996.
4. Vardy A.E., *Aerodynamic drag on trains in tunnels. Part 1: synthesis and definitions*, *Journal of Rail and Rapid Transit*, **210 (1)**, 29-38, 1996.
5. Vardy A.E., *Aerodynamic drag on trains in tunnels. Part 2: prediction and validation*, *Journal of Rail and Rapid Transit*, **210 (1)**, 39-49, 1996.
6. Mossi M., *Swissmetro: strategy and development stages*, Maglev'2002, the 17th International Conference on Magnetically Levitated Systems and Linear Drives, EPF Lausanne, September 2002.
7. Baron A., Mossi M., Sibilla S., *The alleviation of the aerodynamic drag and wave effects of high-speed trains in very long tunnels*, *J. Wind Engineering and Industrial Aerodynamics*, **89**, 365-401, 2001.
8. Baron A., Losi F., Orso F., *Simulazione numerica dei fenomeni aerodinamici prodotti da treni ad alta velocità in tunnel di forma complessa*, *Ingegneria Ferroviaria*, **7**, 3-19, 1996.
9. Sockel E., *The tunnel entrance problem*, Von Karman Institute 1972 Lecture Series, 1-16, 1972
10. Lancien D., Caille P., Parent de Curzon E., Jutard M., *Aspects aérodynamiques de la circulation à grande vitesse en tunnel*, *Revue Générale des Chemins de Fer*, **106**, 5-22, 1987.
11. Woods W.A., Gawthorpe R.G., *The train and tunnel - A large scale unsteady flow machine*, 2<sup>nd</sup> International JSME Symposium on Fluid Machinery and Fluidic, 249-258, Tokyo, 1972.
12. Woods W.A., Pope C.W., *On the range of validity of simplified one-dimensional theories for calculating unsteady flows in railway tunnels*, 3<sup>rd</sup> Int. Symp. on the Aerodynamics and Ventilation of Vehicle Tunnels, Sheffield, 115-150, 1979.
13. Henson D.A., Bradbury W.M.S., *The aerodynamics of Channel tunnel trains*, 7<sup>th</sup> Int. Symp. on the Aerodynamics and Ventilation of Vehicle Tunnels, 927-956, 1991.